

A Picture of Quasi-Ballistic Transport in Nanoscale MOSFETs

Hideaki Tsuchiya, Kazuya Fujii, Takashi Mori and Tanroku Miyoshi

Kobe University, Department of Electrical and Electronics Engineering
1-1, Rokko-dai, Nada-ku, Kobe 657-8501, Japan

Phone & Fax (common): +81-78-803-6082 E-mail: tsuchiya@eedept.kobe-u.ac.jp

1. Introduction

As a channel length of MOSFETs is scaling down to the length scale of a carrier's mean free path, ballistic or quasi-ballistic transport is expected [1]. Understanding physics of the ballistic transport of carriers is important to elucidate a scaling limit of MOSFETs. A schematic diagram representing how to determine a current drive in the quasi-ballistic model is shown in Fig. 1. The source is treated as a reservoir of thermal carriers, which injects carriers from source to the forward channel with an injection velocity of v_{inj} in the case of ballistic limit, and the saturation current I_{sat} is simply given by a product of v_{inj} and injected carrier concentration N_s^{source} . When scattering exists in the channel, an average carrier velocity at the source-channel barrier v_s decreases from v_{inj} and the saturation current is expressed as [1]

$$I_{sat} = qN_s^{source}v_s = qN_s^{source}v_{inj} \times \frac{1-R}{1+R(v_{inj}/v_{back})} \quad (1)$$

where R is a backscattering coefficient and v_{back} a backward channel velocity [1]. The numerator $1-R$ and denominator $1+R(v_{inj}/v_{back})$ in eq. (1) represent the current reduction due to an increase of *backward* moving carriers and a decrease of *forward* moving carriers to keep the total carrier concentration induced by gate bias, respectively. In the ballistic limit ($R=0$), $v_s=v_{inj}$. As far as we're concerned, a physical mechanism creating v_{inj} and roles of scattering in eq. (1) have not been fully understood yet.

In this paper, we discuss v_{inj} and roles of scattering based upon a quantum-corrected Monte Carlo (MC) simulation.

2. Injection Velocity v_{inj}

To investigate a physical mechanism creating v_{inj} , we first performed a ballistic MC simulation, which means that the scattering is neglected in the channel region, while the scatterings in the source and drain are considered. As a simulation model, we adopted a double-gate and ultra-thin body MOSFET ($T_{Si}=3\text{nm}$) to suppress the short channel effect. The quantum effects are considered by using a quantum correction of potential [2]. As scattering processes, impurity scattering, interface roughness scattering, intravalley acoustic phonon and intervalley phonon scatterings, and electron-electron scattering are considered [2]. Fig. 2 shows the electron transport properties computed for fictitious ballistic MOSFETs with various channel lengths. Here, it should be noted that the average electron velocity increases along the channel at the source-channel barrier (potential bottleneck) regardless of L_{ch} , which is due to a carrier diffusion effect caused by a spatial gradient of the concentration $\nabla_r n$ as found in Fig. 2 (a). Namely, v_{inj} is

determined by usual drift-diffusion-like transport even in the ballistic MOSFETs. Fig. 3 shows the momentum distribution function for the ballistic MOSFET with $L_{ch}=30\text{nm}$. It is found that the distribution function changes shape rapidly at the source-end of channel. To examine the shape more closely, the distribution functions at the inside of source and at the potential bottleneck point are shown in Fig. 4 (a) and (b), respectively. Here, the open circles in Fig. 4 (b) indicate an asymmetric Fermi-Dirac function [1]. It is found that the asymmetric Fermi-Dirac function is a good analytical approximation at the high momentum region, but the behavior around zero momentum is quite different.

3. Roles of Scattering

Next, we discuss the roles of scattering. Fig. 5 shows the influence of scattering on the distribution function at the potential bottleneck point, where the real channel includes the scattering. The increase in the negative momentum denotes the presence of backward channel current due to the scattering, while the decrease in the positive momentum is to keep the carrier concentration induced by the gate bias as mentioned in Sec. 1. Further, the index of ballisticity r_B and backscattering coefficient R are calculated as a function of L_{ch} as shown in Fig. 6, where $r_B=I_D(\text{real})/I_D(\text{ballistic})$. It is found that r_B approaches 1.0 and R reduces down to a few % in the sub-10nm regime. We also found that an assumption $v_{back}=v_{inj}$ [3] is invalid. Finally, Fig. 7 shows the N_s^{source} dependences of I_{sat} and v_s for $L_{ch}=8\text{nm}$ MOSFET with scattering. The dashed lines indicate the results from the analytical formulae for perfect ballistic MOSFETs [1]. Since the carrier transport approaches ballistic for $L_{ch}=8\text{nm}$, I_{sat} and v_s are comparable to those from the analytical formulae. However, note that v_s is almost independent of N_s^{source} as opposed to the analytical formulae, which may be related to the drift-diffusion-based carrier transport at the source-end of channel.

4. Conclusions

Based upon the quantum-corrected MC simulation, we proposed a picture of quasi-ballistic transport in MOSFETs, that is, the carrier injection is controlled by a drift-diffusion-like transport, and thus the carrier velocity at the source-end of channel is almost independent of N_s . We also found that the carrier transport approaches ballistic in sub-10nm regime.

Acknowledgements

We would like to thank Prof. Shin-ichi Takagi of University of Tokyo for his valuable discussions.

References

- [1] K. Natori, IEICE Trans. Electron. **E84-C** (2001) 1029.
 [2] H. Tsuchiya, A. Oda, M. Ogawa, and T. Miyoshi, Jpn. J. Appl. Phys. **44** (2005) 7820.
 [3] M. Lundstrom, IEEE Electron Device Lett. **18** (1997) 361.

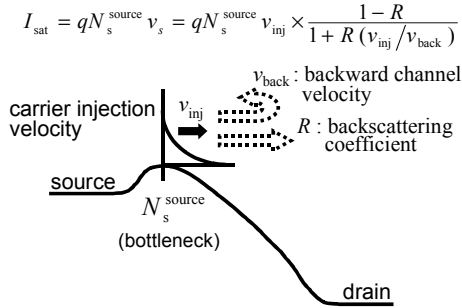


Fig. 1 Schematic diagram representing how to determine current drive in quasi-ballistic model. In the ballistic limit ($R=0$), $v_s = v_{inj}$.

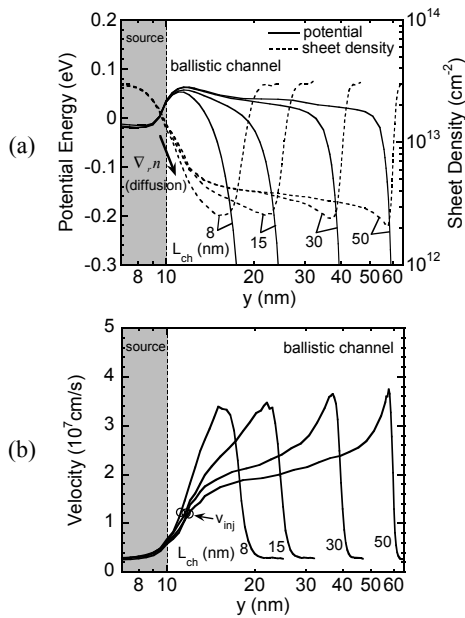


Fig. 2 (a) Potential and sheet electron concentration and (b) average electron velocity profiles along channel computed for ballistic DG-MOSFETs with various channel lengths. $V_{DS}=0.6V$ and V_G is adjusted to keep the sheet electron concentration N_s^{source} equal to $7 \times 10^{12} \text{cm}^{-2}$ at the source-channel barrier. The scattering in the source and drain regions is considered.

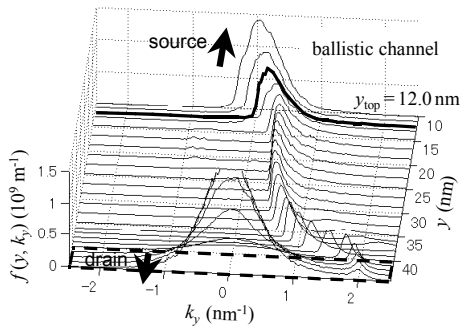


Fig. 3 Distribution function in momentum space computed for ballistic MOSFET with $L_{ch}=30\text{nm}$. The channel region extends from $y=10$ to 40nm . The potential bottleneck is located at $y=12$ nm.

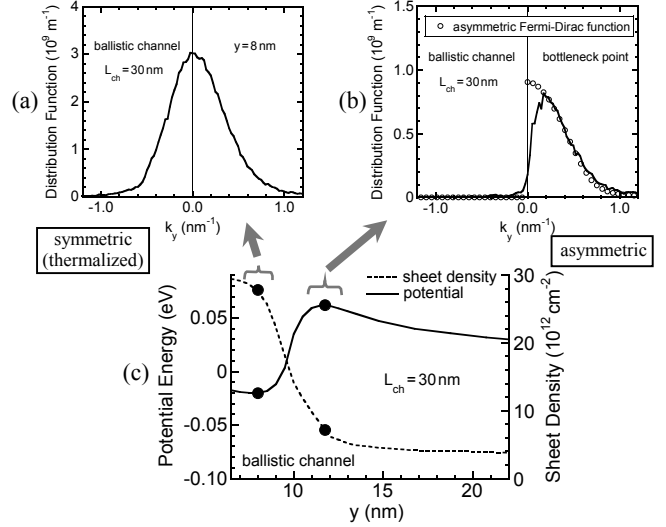


Fig. 4 Distribution functions at (a) $y=8\text{nm}$ (inside of source) and (b) potential bottleneck point of ballistic MOSFET with $L_{ch}=30\text{nm}$. The open circles in (b) denote the asymmetric Fermi-Dirac function. (c) represents the magnified profiles of potential and N_s .

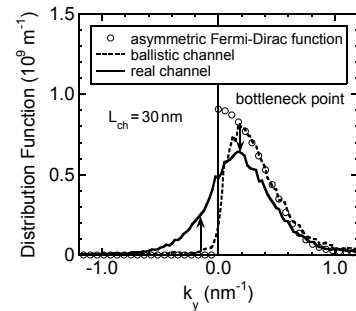


Fig. 5 Change in shape of distribution functions at bottleneck point due to scattering. The real channel includes the scattering.

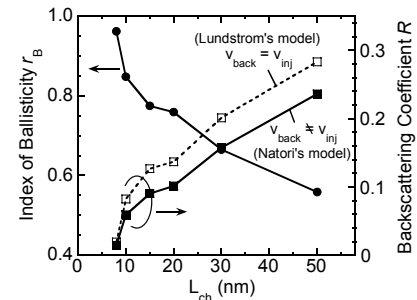


Fig. 6 Index of ballisticity r_B and backscattering coefficient R calculated as a function of L_{ch} . We found $v_{back} \approx 0.5 \sim 0.6v_{inj}$.

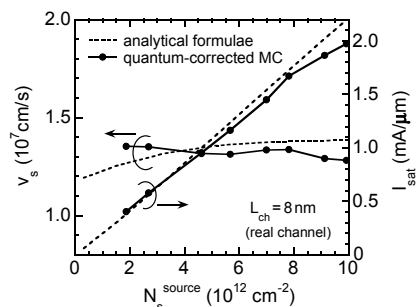


Fig. 7 N_s^{source} dependences of I_{sat} and v_s for $L_{ch}=8\text{nm}$ MOSFET with scattering. The dashed lines indicate the results from the analytical formulae for perfect ballistic MOSFETs[1].